Developing a Sequential Mask Projection Technique for Micro-Lens Generation Using Excimer Laser Micro-Structuring

Eric Syrbe, Sebastian Buettner, Michael Pfeifer and Steffen Weissmantel
Laserinstitut Hochschule Mittweida, Technikumplatz 17, Mittweida, Germany

Keywords: Excimer Laser, Micro-Optics, Micro-Lenses, Fluorine Laser, Direct Laser Fabrication, Micro Machining.

Abstract: Fluorine laser micro-structuring enables the generation of micro-optics in glasses and other wide band gap materials. For the generation of micro-lenses, we developed a new micro-structuring method and the appropriate hardware. The process is based on the mask projection technique and uses a set of different circular masks, which are placed consecutively within the laser beam. This creates a ring-shaped ablation area with variable inner radius. By using an appropriate set of masks, it is possible to generate a surface with a defined spherical shape. The measured radii of curvature of the structured micro-lenses are in the range of 90 µm up to 250 µm with corresponding surface roughness values to below 100 nm. The entire process and requirements are described, and the results are presented.

1 INTRODUCTION AND STATE OF THE ART

Current technical innovations are often based on improved efficiency or a more compact design. The latter case requires a miniaturization of the included parts, which is a constant challenge for the involved manufacturing processes. One of the driving forces behind are the computer and communication technologies, because data transmission via the classic copper cable is limited in terms of transmission speed and becomes more susceptible to electromagnetic interference fields the greater the volume of data transmitted per second. One solution is offered by optical data transmission, which is insensitive to these effects and shows a low signal attenuation, so that signals can be transmitted over long distances with virtually no loss or errors. The coupling of the optical signals into progressively smaller wave guiding structures such as mono mode fibres require micro-optics with best possible shape accuracy and low surface roughness. A wide range of processes was developed to fulfil these demands. Imprinting (Moore, Gomez, & Lek, 2016) and additive techniques (Bückmann, Schittny, Thiel, & Kadic, 2014; Kim, Brauer, Fakhfouri, & Boiko, 2011) are especially used to produce polymer micro-optics. But there is still a great need for development regarding the production of micro-optics in glass materials and in high-quality fused silica, e.g. for integrating optics into a wafer. Only a few processes are still suitable for processing this material, with the most used being lithography. However, the latest developments are increasingly using femtosecond (Hua, Liang, Chen, Juodkazis, & Sun, 2022) and CO_2 lasers (Zhao et al., 2022) or a combination of both (Sohn, Choi, Noh, Kim, & Ahsan, 2019) to achieve the desired lens quality. The approach we have been pursuing for some years now is to use excimer lasers and the mask projection technique for this purpose. It has been successfully demonstrated that a wide variety of micro-optics can be produced using the numerous structuring methods we have developed. But as with the other laser structuring methods the achievable quality is still a major challenge.

In this research we aim to reduce the influence of re-deposition of debris at the ablation area during the patterning process. The previously developed method uses a rotating mask where the debris is always pushed ahead into the following ablation area. This results in irregularities in the structure and its surface (Buettner, Pfeifer, & Weissmantel, 2020). To solve this problem, we have changed the strategy for lens structuring to a full area structuring method in which the ablation area is gradually reduced and always lies within the previous area. Therefore, almost no debris should be found inside the ablation area after structuring. To achieve this gradually changing mask geometry we used a combination of a set of circular masks and an outer aperture.

Syrbe, E., Buettner, S., Pfeifer, M. and Weissmantel, S.
Developing a Sequential Mask Projection Technique for Micro-Lens Generation Using Excimer Laser Micro-Structuring.
DOI: 10.5220/0012377400003651

In *Proceedings of the 12th International Conference on Photonics, Optics and Laser Technology (PHOTOPTICS 2024)*, pages 21-27
ISBN: 978-989-758-686-6; ISSN: 2184-4364

2 EXPERIMENTAL SETUP

2.1 Process

The used system consists of the pulsed fluorine laser LPF 220i of Coherent Lasersystems GmbH & Co. KG and the micro machining station EX-157. A detailed description of the station is given in our previous work (Buettner, Pfeifer, & Weissmantel, 2019), as the system is identical. Due to its beam characteristics the fluorine laser is not suited for the direct-writing technique. Therefore, a mask projection technique is applied. To get the laser pulse fluence H evenly distributed over the mask area the laser beam is homogenized. If the threshold laser pulse fluence of the material to be structured is exceeded the homogenization results in a uniform ablation depth. Both the laser pulse duration and the used laser wavelength influence the threshold laser pulse fluence. The fluorine laser emits photons with a pulse duration of 25 ns and a wavelength of 157 nm, which corresponds to a photon energy of 7.9 eV. The photon energy is of particular interest for the machining of wide band gap materials, as the difference between photon energy and energy band gap has a direct effect on the processing quality. Higher photon energy, in relation to the band gap energy of the material to be structured, results in a better surface quality of the treated material, due to the better absorption conditions. On the other hand, the energy band gap determines which optical material can be used as mask material for the corresponding wavelength of the laser.

As mentioned above, we targeted to realize a whole area treatment, which requires a combination of several masks. More precisely, the goal was to create a ring-shaped ablation area with a variable inner and a constant outer radius. The inner radius of the ablation area is controlled by a set of special circular masks. The fabrication of the masks is described in the following subsection.

2.2 Mask Generation

As mentioned, the masks must be transparent for the wavelength of the laser. We choose calcium fluoride as mask substrate material, because its band gap energy of 12.2 eV is higher than the photon energy. Therefore, the material is transparent for the used laser wavelength. The 50 mask substrates have a diameter of 5 mm and a thickness of 0.5 mm. The latter is very low, so that hardly any losses occur. To obtain an inner boundary of the ring-shaped ablation area, it is necessary to generate an opaque area on the mask substrate. We used a pulsed laser deposited tantalum coating for this purpose. The main challenge in generating these opaque areas is to position them very precisely on the substrate. For the generation of micro-lenses, these areas are circles with different radii and these circles must each be concentric to the substrate. To solve this problem of precise positioning, a mask holder for the coating process was developed.

The holder consists of three metal plates, the back plate, the sample plate, and the front plate with the sample plate being pinched between the other two plates. The sample plate is a 0.5 mm thick metal plate with 56 holes of 5 mm diameter each so that the calcium fluoride substrates fit ideally into these holes. Other than the back plate, the front plate also got 56 holes of 4 mm diameter to expose one face of the substrates for coating. To change the area to be coated, an additional thin tantalum foil is placed between the sample and the front plate. In this foil, holes with different diameters were cut using an ultra-short pulse laser. In the whole assembly the sample plate, the tantalum foil and the front plate were aligned and fixed on the back plate.

All three plates have adjusting holes for a precise positioning using dowel pins. The adjusting holes ensure that all coating areas are concentric regarding the boundary of each substrate. Following, the pulsed laser deposition coating process is applied to the assembly. In Figure 1 the coated calcium fluoride substrates are shown. Due to the coating mask (tantalum foil) geometries, every area has an individual inner radius generating ablation areas with a radius starting from 1 µm up to 50 µm in 1 µm steps as there are 50 different masks.

Figure 1: Coated calcium fluoride substrates on the sample plate after the pulsed laser deposition coating process, with the front plate and the coating mask removed.

2.3 Hardware

The sequential ablation of material with different mask geometries requires the fast change of the masks within the laser beam. For this a mask wheel was developed, shown in Figure 2.

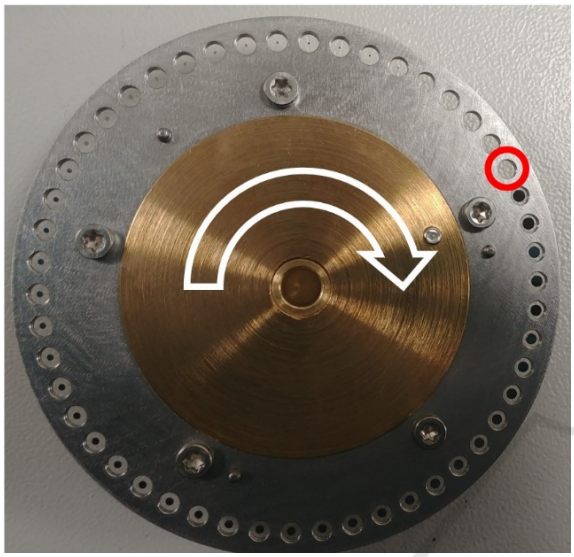

Figure 2: Mask wheel (red: smallest mask, white: direction of rotation).

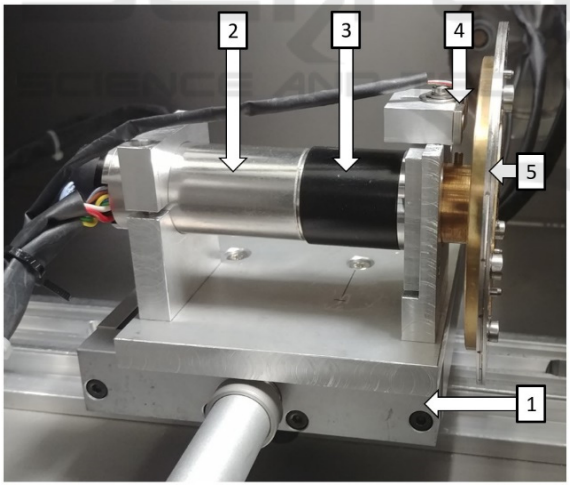

Figure 3: Experimental setup consisting of: linear stage (1), stepper motor (2), 33:1 gear (3), Hall sensor (4) and mask wheel (5).

The coated substrates are again held using three laser-cut plates: a front and back plate with holes of 4 mm diameter and an intermediate plate with holes of 5 mm diameter. These 4 mm holes are responsible for the fixed outline of each micro-optic and are as such the before mentioned constant radius aperture. The holes in the mask wheel are placed on a circle with a radius of 50 mm.

The mask wheel is driven by a servo motor with a 33:1 gear. The used motor encoder has a precision of 4000 increments per revolution. Furthermore, a Hall sensor is added to reference the rotary movement (homing). Now the center of each mask can be moved precisely to the same position within the laser beam. This is important for the position of the ablation areas, and therefore for the geometry of the target structure. The whole assembly, shown in Figure 3, is placed on a linear stage, which is used for adjusting the wheel position to the laser beam height.

2.4 Calculation of the Process Parameters

In principle, two different process methods are possible. In method 1, the mask wheel is rotated during the structuring process at a speed that is synchronised with the laser pulse repetition rate. Thus, a micro-optic can be completed in about 0.25 s if all 50 masks are used, and the laser emits at its maximum pulse repetition frequency of 200 Hz. However, this method requires a mask set specially made for the micro-optics to be structured. This mask set then enables the fast industrial production of identical lenses.

In method 2, the rotary motion is stopped at each mask position and the calculated number of laser pulses needed to form the target structure is applied. Due to the acceleration and deceleration of the mask wheel the processing times are about one minute per micro-optic, which is significantly slower than method 1. On the other hand, this second method is more flexible since a mask can be used several times and thus more masks with different diameters fit into the mask wheel. Since many different micro-lenses are to be structured, the second method is used for this study.

The number of laser pulses and the necessary set of masks are calculated using a variance comparison. The starting point of each calculation is the target radius of curvature (ROC) and the given laser pulse fluence which determines the ablation depth per laser pulse Δz. As the lens is rotationally symmetrical the calculation can be simplified to two dimensions. The centre of the lens is always at a radius of $r = 0$ µm. The target profile is then defined by a circle equation with the target ROC. The calculation of the actual profile starts with the radius value $r_{m,1}$ corresponding to the first mask in the mask set being used. The required ablation depth for each mask radius r_m is the difference between the profile depth for the current

mask radius, e.g. $r_{m,1}$, and the profile depth for the previous mask radius, e.g. $r_{m,0}$. The number of laser pulses results from the integer rounded ratio of the necessary ablation depth to follow the target profile and the ablation depth per laser pulse Δz. The result of this step-by-step calculation procedure is shown as an example in Figure 4.

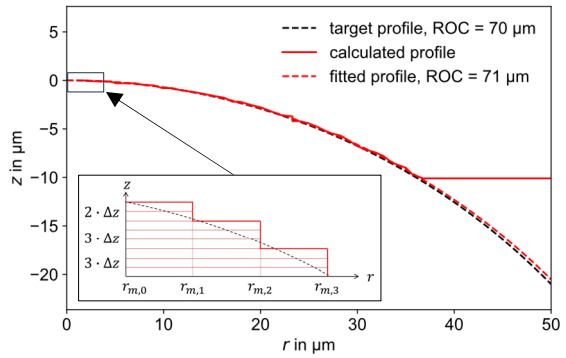

Figure 4: Exemplary result of a variance comparison calculation for a given target profile.

3 RESULTS

We used laser pulse fluences from $H = 0.5$ J/cm^2 up to 2.0 J/cm^2 and target ROC from 50 µm up to 250 µm to determine the optimal parameter set for each target structure. In principle, the setup described in the previous chapter enables the generation of micro-lenses, as demonstrated by the example in Figure 5.

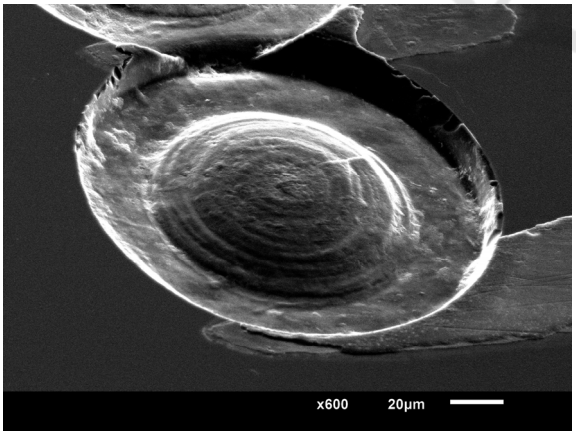

Figure 5: Scanning electron microscope picture of a micro-lens with $H = 1.0$ J/cm^2 and a ROC of 250 µm.

After the structuring process the micro-lenses are measured with a laser scanning microscope. The height data is then analysed using a python program that fits a sphere to the data with the radius as the variable fit parameter. This radius is the measured ROC. Each parameter set was structured three times to evaluate the process stability. In the following figures every point represents the result for one micro-lens.

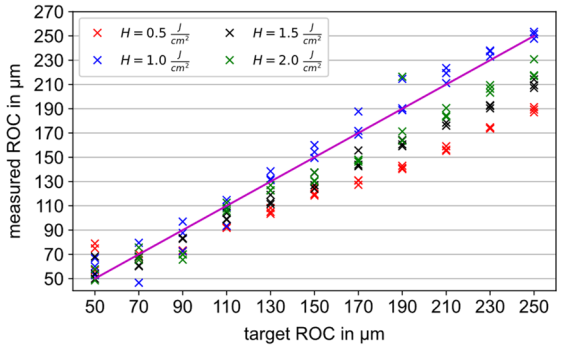

Figure 6: Comparison of the measured ROC to the target ROC of the lens structures for different laser pulse fluences. The magenta line indicates the ideal ROC.

Figure 6 shows that the measured ROC of the structures with $H = 1.0$ J/cm^2 deviate the least from the target ROC with one structure from each parameter set almost exactly showing the target ROC. For the other laser pulse fluences the measured ROC is significantly smaller. The ratio between measured and target ROC remains approximately constant for all parameter combinations: $H = 0.5$ J/cm^2: 0.75; $H = 1.5$ J/cm^2: 0.84; $H = 2.0$ J/cm^2: 0.88. These constant deviations point to an error regarding the laser pulse fluence measurement which could be minimised by applying a correction factor for each laser pulse fluence. This factor can be iteratively adjusted by structuring a series of lenses with different target ROC and calculating the ROC deviation.

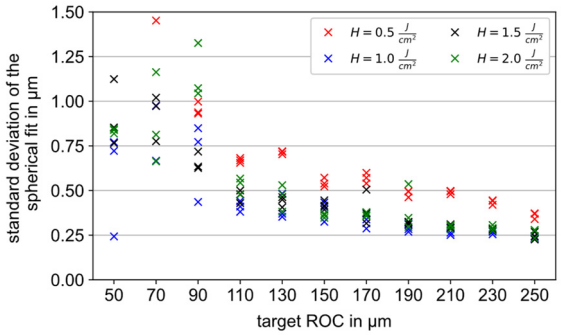

Figure 7: Standard deviation of each spherical fitted ROC for every structured micro-lens.

The calculation of the standard deviation for each fitted sphere, as shown in Figure 7, can be used as an

indicator for the shape accuracy of each lens. It can be noticed that larger target ROC values result in lower standard deviations. The lenses structured with H = 1.0 J/cm² generally show the lowest standard deviations meaning that they correspond most closely to the shape of an ideal sphere. The lenses with H = 1.5 J/cm² and H = 2.0 J/cm² show values of standard deviation that are just a bit higher. The H = 0.5 J/cm² lenses generally show the highest standard deviations. In addition to being the farthest away from the target ROC, this laser pulse fluence is thus not suitable for structuring useful micro-lenses.

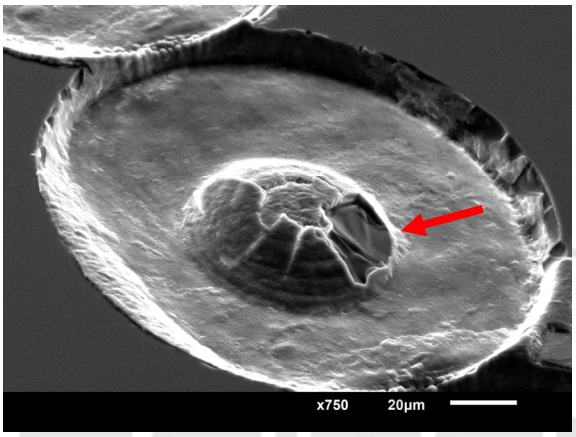

Figure 8: Scanning electron microscope picture of a micro-lens with H = 1.0 J/cm² and a ROC of 50 µm. The red arrow points at the clearly visible chipping.

Small values of target ROC result in high standard deviations, because those lenses tend to chip making them useless as an optical device. An exemplary micro-lens is shown in Figure 8. The chipping is also the reason for the measured ROC deviation for the smallest target ROC of 50 µm and 70 µm, as shown in Figure 9.

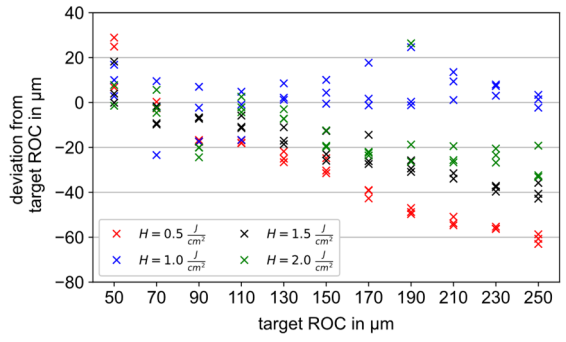

Figure 9: Deviation of the measured ROC from the target ROC for different laser pulse fluences.

However, the chipping does not occur in any micro-lens with a ROC of 90 µm and larger. This structuring method can therefore be used to produce micro-lenses with a radius of curvature ≥ 90 µm. Figure 9 again shows that the laser pulse fluence of H = 1.0 J/cm² is most suited for the generation of micro-lenses closest to a given target ROC. To further analyze these lenses regarding the repeatability of the structuring process the deviation from the mean measured ROC for each target ROC can be calculated. The result is shown in Figure 10. The lenses with a target ROC of 70 µm and 190 µm show the largest deviation with 18 µm and 16 µm respectively. The smallest deviation occurs with the lenses with the largest target ROC of 230 µm and 250 µm with 3 µm each. This corresponds to a deviation from the mean measured ROC of about 1 % which indicates a good repeatability of the structuring results for the respective process parameters.

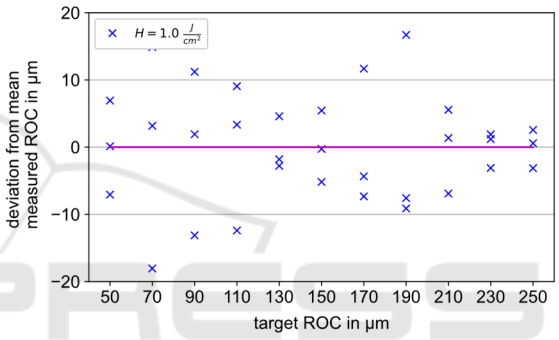

Figure 10: Deviation from the mean measured ROC for each target ROC using a laser pulse fluence of H = 1.0 J/cm². The magenta line indicates an ideal deviation of 0 µm.

The laser pulse fluence of H = 1.0 J/cm² also results in the smallest overall root mean square surface roughness values at around S_q = 80 nm, as shown in Figure 11. This value is obtained by convolving the height data with a gaussian filter using a standard deviation value corresponding to a defined cutoff wavelength of λ_c = 8 µm. Overall S_q is decreasing by increasing target ROC. The reason for this is that fewer laser pulses per mask position are required to produce micro-optics with a larger ROC. The surface roughness for all target ROC greater than 170 µm is generally below 130 nm which in relation to the design wavelength for optical data transmission of 1310 nm equals λ/10. The so far best shape lenses are those structured with the laser pulse fluence of H = 1.0 J/cm². To further analyse their surface roughness different cutoff wavelengths can be used for the calculation, as shown in Figure 12 with λ_c = (2.5; 8.0; 25) µm. The smaller the cutoff value the lesser the roughness. For the ROC of 250 µm the three roughness values for the corresponding cutoff

wavelengths of (2.5; 8.0; 25) µm are (38; 74; 172) nm respectively. 38 nm is less than $\lambda/30$ in relation to the design wavelength.

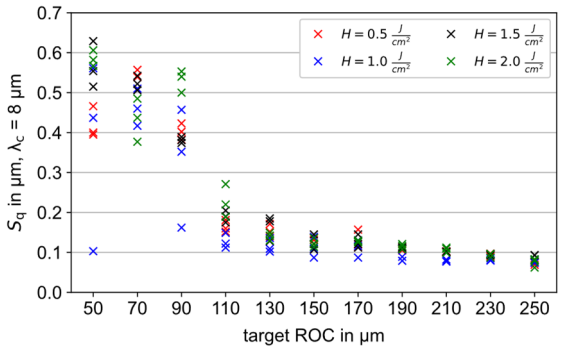

Figure 11: Calculated surface roughness S_q for every structured lens using a cutoff wavelength of 8 µm.

Yet another way of assigning a roughness value to each structure is already given in Figure 7 through the standard deviation of each spherical fitted ROC. These values can be interpreted as the roughness that remains when the ideally fitted lens shape is subtracted from the measured height data as the formula for the standard deviation is identical to the formula for surface roughness. But these roughness values do not involve a specific cutoff wavelength, they are rather an indication of the wavefront error a plane wave would get when passing through the micro-lens.

Ultimately the calculation and the needed surface roughness value is dictated by the application the micro-optics are used for.

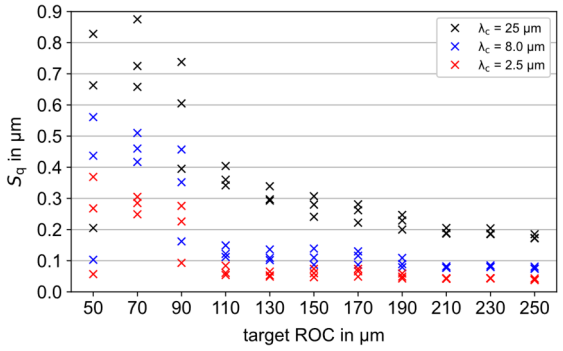

Figure 12: Calculated surface roughness S_q for all lenses structured with a laser pulse fluence of H = 1.0 J/cm^2 using three different cutoff wavelengths.

Regarding a process optimisation, there are two possible starting points. Firstly, we detected a mask misalignment error while evaluating the generated micro-lenses, as shown exemplary in Figure 13. This error can be a result of backlash in the motor gearbox which could be solved by attaching the motor encoder directly onto the mask wheel. The error could also be caused due to misalignment during the fabrication of the mask wheel or during the mounting of the mask wheel to the motor axis. Both could result in the masks not being concentric to the motor axle which would explain the mask misalignment. Solving this problem would lead to lenses that are closer to the ideal shape of a sphere and simultaneously also smoother, depending on the used roughness calculation method.

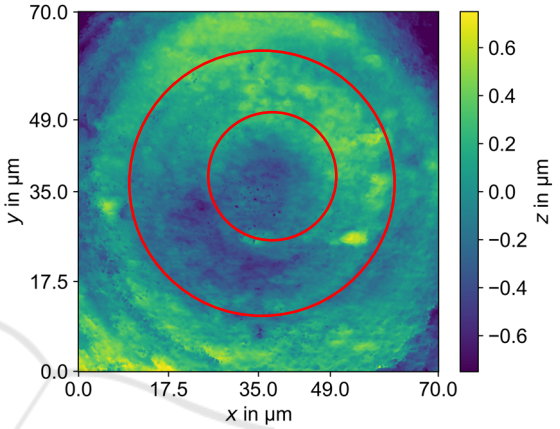

Figure 13: Mask misalignment error. The red circles indicate the inner edge of two ablation areas that are not ideally concentric.

Secondly, the fluorine laser slowly loses power while not emitting at a its maximum pulse repetition frequency of 200 Hz. As the mask wheel has to stop at each mask position to wait until the necessary number of laser pulses is applied, the effective pulse repetition frequency is much lower than 200 Hz. As a result, the laser pulse fluence slowly decreases with increasing duration of the structuring process. This has a particular effect on the ablation areas with the largest inner radius because these are processed last. Therefore, once an optimal parameter set for a specifically needed target ROC is found, the next step is to reduce the total process time by using only the necessary masks and applying process method 1 as described in section 2.4. This should further decrease the local deviations from the ideal lens shape as the laser can now operate close to or even at its maximum pulse repetition frequency.

4 CONCLUSIONS AND OUTLOOK

The combination of sequential mask projection and fluorine laser micro-structuring enables the generation

of rotationally symmetrical micro-optics. For this purpose, the necessary masks were produced and the experimental setup with a rotating mask wheel was built. Each micro-optic to be structured is defined by the used laser pulse fluence and a structure parameter such as the target radius of curvature of a lens geometry. The required mask sequence and the number of laser pulses per mask are calculated using a variance comparison. The evaluation of the structures produced with the calculated parameter sets shows that the calculation method leads in principle to the generation of micro-lenses close to the target geometries. The measured radii of curvature of the micro-lenses produced with a laser pulse fluence of $H = 1.0$ J/cm^2 deviate the least from the respective target radius of curvature. One structure from each parameter set almost exactly matches the predefined target radius of curvature. The surface roughness S_q of those structures decreases with larger target radius of curvature. The smallest calculated S_q values are around 80 nm using the cutoff wavelength of $\lambda_c = 8$ µm.

Our next studies aim to reduce the process time per micro-optic with a different motor-gear-combination as well as the surface roughness by applying a laser smoothing process as an aftertreatment.

REFERENCES

Bückmann, T., Schittny, R., Thiel, M., & Kadic, M. (2014). On three-dimensional dilational elastic metamaterials. New Journal of Physics, 16(3).

Buettner, S., Pfeifer, M., & Weissmantel, S. (2019). Manufacturing of Cylindrical Micro Lenses and Micro Lens Arrays in Fused Silica and Borosilicate Glass using F2-Laser Microstructuring. In M. Raposo, P. A. Ribeiro, & D. Andrews (Eds.), PHOTOPTICS 2019 (pp. 66–72). Setúbal, Portugal: SCITEPRESS - Science and Technology Publications Lda.

Buettner, S., Pfeifer, M., & Weissmantel, S. (2020). Fabrication of Micro Spiral Phase Plates in Fused Silica using F2-Laser Microstructuring. In P. Albella (Ed.), PHOTOPTICS 2020 (pp. 114–121). Setúbal: SCITEPRESS - Science and Technology Publications Lda.

Hua, J.-G., Liang, S.-Y., Chen, Q.-D., Juodkazis, S., & Sun, H.-B. (2022). Free‐Form Micro‐Optics Out of Crystals: Femtosecond Laser 3D Sculpturing. Advanced Functional Materials, 32(26).

Kim, J. Y., Brauer, N. B., Fakhfouri, V., & Boiko, D. L. (2011). Hybrid polymer microlens arrays with high numerical apertures fabricated using simple ink-jet printing technique. Optical Materials Express, 1(2), 259.

Moore, S., Gomez, J., & Lek, D. (2016). Experimental study of polymer microlens fabrication using partial-filling hot embossing technique. Microelectronic Engineering, 162, 57–62.

Sohn, I.-B., Choi, H.-K., Noh, Y.-C., Kim, J., & Ahsan, M. S. (2019). Laser assisted fabrication of micro-lens array and characterization of their beam shaping property. Applied Surface Science, 479, 375–385.

Zhao, L., Cheng, J., Yin, Z., Yang, H., Liu, Q., Tan, C., et al. (2022). Rapid CO 2 laser processing technique for fabrication of micro-optics and micro-structures on fused silica materials. Proceedings of the Institution of Mechanical Engineers, Part B: Journal of Engineering Manufacture, 236(1-2), 100–110.